Optics Letters

Photonic analog-to-digital conversion with equivalent analog prefiltering by shaping sampling pulses

Feiran Su, Guiling Wu,* and Jianping Chen

State Key Laboratory of Advanced Optical Communication Systems and Networks, Department of Electronic Engineering, Shanghai Jiao Tong University, Shanghai 200240, China
**Corresponding author: wuguiling@sjtu.edu.cn*

Received 14 April 2016; revised 10 May 2016; accepted 17 May 2016; posted 17 May 2016 (Doc. ID 263119); published 9 June 2016

We propose a photonic scheme to digitize RF signals with a programmable equivalent analog prefilter, where the filter impulse response is directly proportional to the time-reversed temporal shape of the sampling pulse and hence can be adjusted by shaping sampling pulses. The model of the proposed scheme is presented to prove its principle and derive its operation conditions. A four-channel scheme with program-controlled pre-filters is demonstrated experimentally, where bandpass filters with the phase shifts of 0°, 90°, 180°, and 270° are synthesized, respectively, by changing temporal shape of the sampling pulses. The experimental results agree well with the theoretical analysis, indicating the validity of the proposed scheme. © 2016 Optical Society of America

OCIS codes: (060.5625) Radio frequency photonics; (320.0320) Ultrafast optics; (320.5540) Pulse shaping.

http://dx.doi.org/10.1364/OL.41.002779

Photonic analog-to-digital converters (ADCs), benefiting from the merit advantages of photonics, have the potential to break the bottlenecks of electronic ADCs in bandwidth and aperture jitter to directly digitize RF signal, and may find important applications in communications, modern radars, and instrumentation, etc. [1]. During the past decades, several schemes have been proposed [2–4] to improve the performance of photonic ADCs in terms of sampling rate, input bandwidth, and effective number of bits (ENOB). In many applications an analog prefilter prior to ADC is often required for various purposes, such as antialiasing, suppressing interference, and shifting phase. Conventionally, electronic analog filters are used to fulfill the purposes. However, electronic analog filters have several limitations in bandwidth, loss and, tunability [5]. Microwave photonic filters (MPFs) have been proposed to overcome these limitations [5]. Using a MPF as the prefilter of photonic ADCs seems to be a compatible choice. However, the direct cascade of a MPF and a photonic ADC needs multistages electro-optic and optic-electric conversion, which will result in significant loss and distortion.

In this Letter, we propose a photonic scheme to digitize RF signals with a programmable equivalent analog prefilter by shaping photonic sampling pulses. The proposed scheme has a similar structure to time-interleaved photonic ADCs (TIPADCs) where each sampling channel can be modeled as an analog filter along with a sampler [6]. The analog filter can be considered as the equivalent prefilter whose response is the same as the channel response of TIPADCs. Based on the fact that the channel impulse response of TIPADCs is proportional to the product of the time-reversed temporal shape of the sampling pulse train and the photodetection impulse response [6], we reveal that the prefilter impulse response can be directly proportional to the time-reversed temporal shape of the sampling pulse under certain conditions. In the case, by shaping the sampling pulse, the impulse response of the equivalent prefilter can be directly controlled. When multiple channels are interleaved together to increase the total sampling rate, all the prefilters in channels are combined to form a global equivalent prefilter accordingly. Compared to traditional MPFs, the equivalent prefilter has the same advantages, such as wideband, flexibility, and reconfigurability. However, the proposed scheme directly obtains the filtered and digitized result while it does not output any filtered analog result. Moreover, the bandwidth of the photodetection in the proposed scheme can be much lower than the frequency of the RF input while it must be not less than the frequency of the RF input in existing MPFs. A four-channel scheme based on the principle is demonstrated. By shaping the sampling pulse, bandpass prefilters are synthesized, and the phase shifting ability is also illustrated to validate the flexibility and reconfigurability of the scheme.

Figure 1 shows the schematic of the proposed scheme. A shape-controlled photonic sampling pulse train generated by a pulse source is modulated by an input RF signal via an intensity modulator. The modulated photonic pulses are demultiplexed into N channels to be photodetected and digitized in parallel by electronic ADCs. The filtering is underlying in the whole process and the samples in each channel are the result of filtering and digitizing the RF input, which can be combined to reconstruct the prefiltered RF signal.

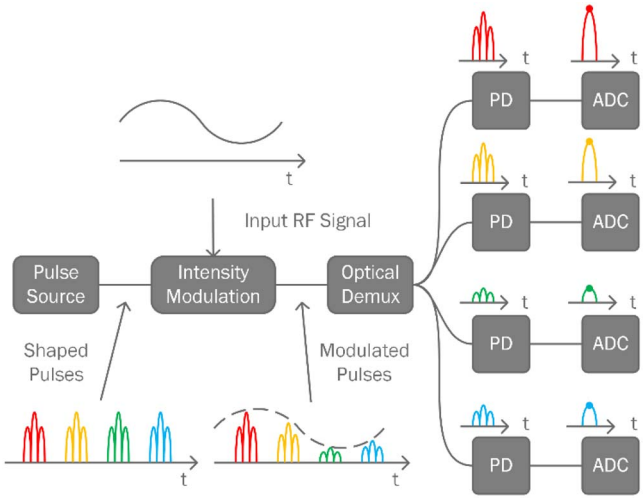

Fig. 1. Schematic of the proposed scheme. PD, photodetection.

We can consider the pulse train is interleaved by N subtrains, each of them corresponds to a demultiplexing channel. The temporal shape of the n-th subtrain can be expressed as

$$p_n(t) = P_{A,n} \sum_{m=-\infty}^{\infty} p_{S,n}(t - mT_S - d_{P,n}), \tag{1}$$

where $P_{A,n}$ is the average power of the n-th subtrain, $p_{S,n}(t)$ is the sampling pulse temporal shape normalized by $P_{A,n}$, T_S is the pulse repetition period, and $d_{P,n}$ is the delay of the n-th subtrain.

For intensity modulation in the small-signal condition adopting a Mach–Zehnder modulator (MZM) biased at quadrature, the samples in the n-th channel sampled by an electronic ADC with the sampling rate of $f_S = 1/T_S$, $v_{Q,n}[k]$, can be expressed as [6]

$$v_{Q,n}[k] = 0.5\alpha_n h_{E,n}(t - d_{E,n}) * p_n(t)|_{t=0} + h_{A,n}(t) * v_I(t)|_{t=kT_S}, \tag{2}$$

where α_n is the attenuation factor of the MZM to the n-th subtrain, $h_{E,n}(t)$ is the photodetection impulse response accounting from the photodiode to the electronic ADC, $d_{E,n}$ is the delay added in the photodetection, and $v_I(t)$ is the input RF.

In Eq. (2), the first term, denoted as $V_{Q0,n}$, is a constant; the second term $v_{Q1,n}[k]$ is the response of the n-th channel to the input, and $h_{A,n}(t)$ characterizes the channel response,

$$h_{A,n}(t) = -0.5\alpha_n h_{M,n}(t) * [h_{E,n}(t - d_{E,n})p_n(-t)], \tag{3}$$

where $h_{M,n}(t)$ is the small-signal impulse response of the MZM. From Eq. (2), the proposed scheme can be described by an equivalent model, shown in Fig. 2, with an equivalent analog filter of $h_{A,n}(t)$ prior to sampling in each channel.

In Eq. (3), the effect of the modulator is equivalent to a cascade filter, and can be investigated independently. In addition to the modulator, we can find that $h_{A,n}(t)$ is determined by the product of $p_n(-t)$ and $h_{E,n}(t - d_{E,n})$. From this point, $h_{A,n}(t)$ can be just proportional to a delayed $p_{S,n}(-t)$ in theory if just one of the pulses in $p_n(-t)$ is left in the product. That is, in each channel, the impulse response of the prefilter is just proportional to the time-reversed sampling pulse temporal

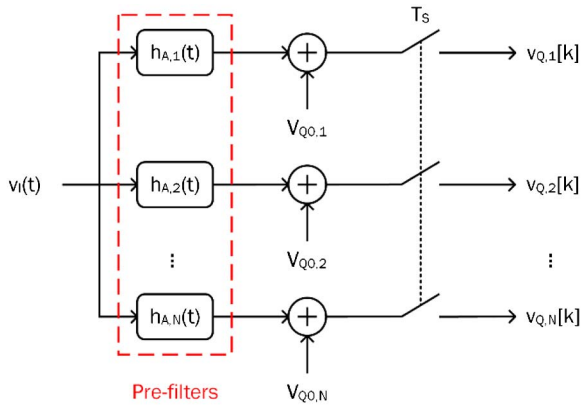

Fig. 2. Equivalent model of an N-channel scheme.

shape. Specifically, the conditions resulting in the above case can be described as follows and illuminated in Fig. 3. From Fig. 3, we can see that $h_{E,n}(t)$ can select only a single pulse out when we have

$$w_P < w_E < T_S, \tag{4}$$

where w_E and w_P are the widths of $h_{E,n}(t)$ and $p_{S,n}(t)$, respectively. At the same time, $d_{P,n}$ and $d_{E,n}$ should be appropriate such that the window of $h_{E,n}(t)$ is aligned to one of the pulses of $p_n(-t)$. Once Eq. (4) is satisfied, we can always find the $d_{P,n}$ and $d_{E,n}$. Then a prefilter with an impulse response width less than that of photodetection can be synthesized by shaping the sampling pulse.

The above procedure can be considered as the sampling and reconstruction in the frequency domain, where the spectrum of the pulse train is the sample of the single pulse spectrum with the sampling rate f_S, see Fig. 3. The frequency response of the prefilter is the reconstruction of the single pulse spectrum with delays from the samples, i.e., the spectrum of the pulse train. This procedure and the conditions are similar to reconstructing an analog signal from its digital samples based on the sampling theorem. In the proposed scheme, a frequency response is reconstructed, instead of a time-domain signal.

In principle, the scheme with only one channel can work for the filtering and sampling. However, a system with multiple interleaved channels can increase the total sampling rate,

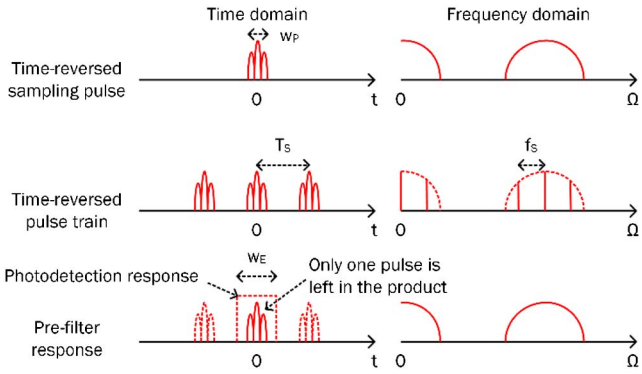

Fig. 3. Diagram of the conditions resulting in that the impulse response of the prefilter is proportional to the time-reversed temporal shape of a single sampling pulse.

and will be more attractive in practice. For the desired interleaving with the matched channel delays and gains, without loss of generality, we have

$$h_{A,n}(t) = h_{A,1}\left(t + \frac{n-1}{N}T_S\right), \tag{5}$$

where $d_{P,n} = (n-1)T_S/N$, $d_{E,n} = (N-n+1)T_S/N$. In this case, samples can be directly interleaved together. Then the total sampling rate is increased by a factor of N while there is a global prefilter $h_A(t)$ prior to the interleaved sampling, $h_A(t) = h_{A,1}(t)$.

Similar to the conventional TIPADC, the highest input frequency of the proposed scheme is determined by the upper bandwidth limit of $h_{A,n}(t)$, which is limited by the modulator bandwidth and the minimum feasible pulse width [6], while its highest input bandwidth is determined by the total sampling rate at which aliasing can be avoided. The photodetection bandwidth also just needs to be not less than half of the single channel sampling rate [6], and the bandwidth bottleneck of electronics can be alleviated effectively by using multiple channels.

Figure 4 shows the experiment setup with four channels. A mode-locked laser (MLL) generates a pulse train with a 36.5 MHz repetition rate and 40 nm linewidth. These pulses are fed into a four-channel programmable wave shaper (Finisar, 4000S) to shape their spectrum. In each channel, an optical delay line (ODL) and a Faraday rotate mirror are used to add a proper delay and reflect pulses back. The pulses from the wave shaper are passed through a 1.7 km dispersion compensating fiber (DCF) (−140 ps/nm/km at 1550 nm) to map the optical spectrum of each pulse to its temporal shape through wavelength-to-time mapping [7]. By changing the optical spectrum shape of the pulses through programming the response of the wave shaper, the pulse train with the repetition rate of ∼146 MHz and the designed shapes can be generated. An erbium-doped optical fiber amplifier along with an optical filter is used to amplify the pulse train. The optical spectrum and the temporal shape of the pulse train are measured by an optical spectrum analyzer (Yokogawa, AQ6370C) and a 70 GHz sampling oscilloscope (OSC) (Keysight, DCA-X 86100D with 86118A module) along with a 95 GHz photodetector (Finisar, XPDV4120R), respectively. A 30 GHz MZM biased at quadrature with a half-wave voltage of 4.5 V is used to modulate the generated pulse train by the single tone RF signals from a microwave signal generator (Rohde & Schwarz, SMF 100A). The power level of the RF input is set at 0 dBm to avoid the MZM nonlinearity [8]. The modulated pulse train is divided into four wavelength channels via a 200 GHz wavelength division demultiplexer. The demultiplexed pulse trains in different channels are aligned via ODLs, and detected by photodetectors (PDs) with 100 MHz bandwidth. Each PD is followed by a second-order Butterworth low-pass filter (LPF) with a 74 MHz bandwidth. A multichannel digitizer with an analog bandwidth of 650 MHz and an ENOB of 9.0 (Keysight, M9703A) is used to sample the photodetected pulses in all channels simultaneously. The synchronizing output of the MLL is fed into a phase-locked circuit (Texas Instruments, LMK04828) to generate the clocks for the digitizer (42 times of the pulse repetition rate, ∼1.53 GHz) and OSC (the pulse repetition rate, ∼36.5 MHz), respectively. The output of the digitizer is downsampled by 42 to obtain one sample per pulse.

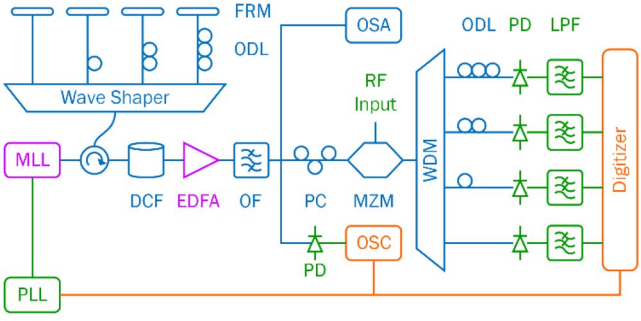

Fig. 4. Experiment setup for a four-channel scheme. EDFA, erbium-doped fiber amplifier; OF, optical filter; PC, polarization controller.

In each channel, since the bandwidth of the adopted PD and digitizer are higher than that of the LPF, the photodetection response is mainly determined by the LPF, which is shown in Fig. 5(b). We can see that when sampling at the peak with the pulse repetition period, intersymbol interference can be ignored, i.e., the condition $w_E < T_S$ is satisfied. The 1 dB width of the response is ∼2.08 ns. Therefore, as long as the width of the optical pulse is less than 2.08 ns, the condition of Eq. (4) is satisfied.

For demonstrating bandpass prefilters, the pulse shape $p_{S,n}(t)$ is controlled by programming the response of the wave shaper to be the product of a cosine function and a Gaussian function. The period of the cosine function is ∼0.18 nm, the 3 dB width of the Gaussian function is ∼0.67 nm, and the channel linewidths are limited to ∼1.23 nm. Figure 5(a) shows the configured response of the wave shaper and the measured optical spectrum of the generated sampling pulse train. Since the pulses are twice filtered by the wave shaper, the attenuation is doubled and the 6 dB width of its spectrum envelope in each channel is ∼0.67 nm. Figure 5(c) shows the measured temporal

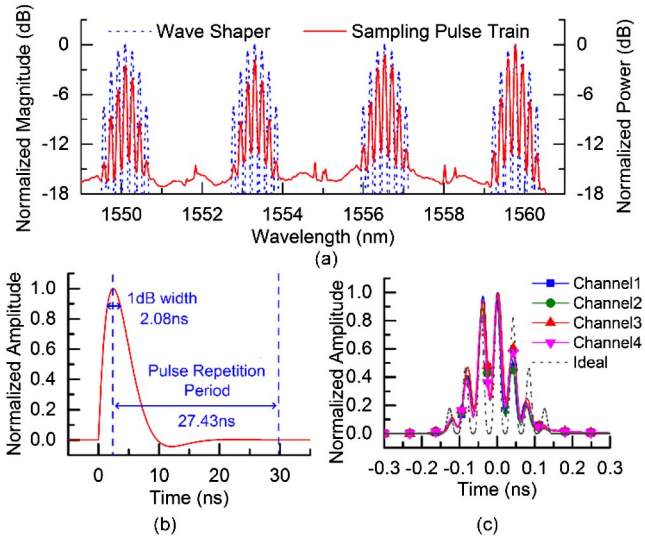

Fig. 5. (a) The response of wave shaper and the measured optical spectrum of the generated sampling pulse. (b) The theoretical impulse response of photodetection in the experiment. (c) The measured temporal shapes of the generated sampling pulse in all channels.

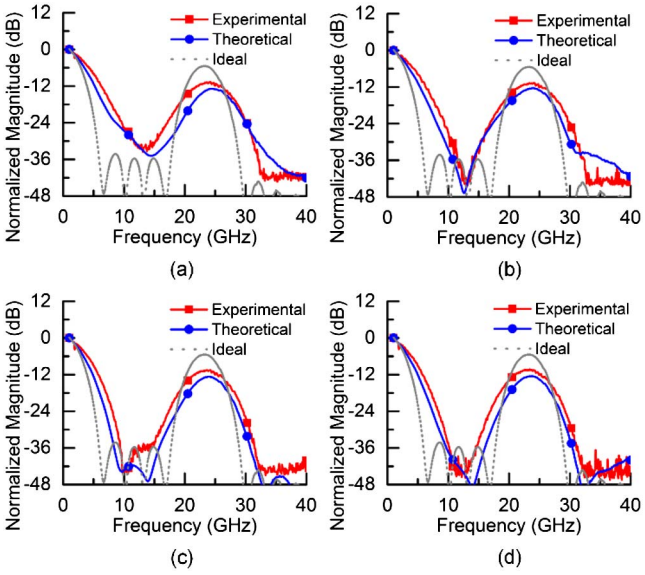

Fig. 6. Amplitude responses of four channels.

shapes of the generated pulse after the DCF in all channels and the ideal temporal shape calculated according to the response of the wave shaper and the parameters of the DCF. Comparing the measured shapes to the ideal one, the periods of the oscillation and the widths of the envelope are consistent while the measured shapes are skewed. This error may originate from the inconsistency of the laser spectrum and the DCF dispersion in different wavelengths.

Figure 6 shows the experimental, the theoretical, and the ideal amplitude-frequency responses of each channel. The theoretical filter responses are calculated from the measured pulse shapes and the response of the MZM according to Eq. (3). The ideal one is calculated as the theoretical one except the measured pulse shape is replaced by the ideal pulse shape. We can see that the experimental and the theoretical ones are consistent. The mismatches among channels and the error to the ideal response are caused by the mismatches of the generated pulses among channels and the error of the pulse shape to the ideal one, respectively, as Fig. 5(c) shows.

The phase responses of the channels relative to channel 1 are measured and shown in Fig. 7(a). One can see that the phase responses are basically linear, which implies that there is no phase distortion in the passband among channels. The relative delays of channels 2–4 to channel 1 estimated by the least-square fitting are 6.89, 13.76, and 20.58 ns, respectively. The deviations to the desired delay under the ideal interleaving are 32, 45, and 7 ps, respectively.

To validate the flexibility and reconfigurability, the phase shifting ability of the prefilter is demonstrated by reconfiguring channel 2. Specifically, the phase of the cosine function in the configuration of the wave shaper response is changed via programs. Since the dispersion of the DCF is negative, a corresponding inverse phase shift will be introduced into the generated sampling pulse after the DCF. Considering the response of the filter is directly equal to the time-reversed temporal shape of the sampling pulse, the phase of the filter should be shifted with the phase change of the cosine function. Figure 7(b) illustrates the measured phase shifts in channel 2

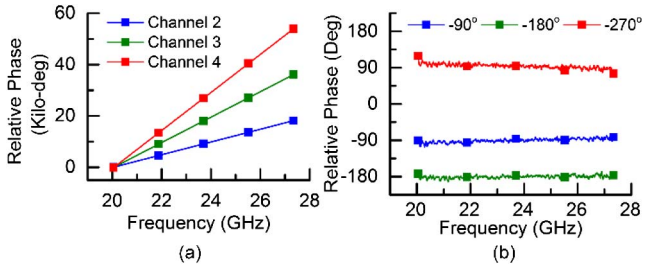

Fig. 7. (a) The measured relative phase responses relative to channel 1. (b) The measured relative phase shift in channel 2 under different phase configurations of sampling pulses.

when the phase of the cosine function is shifted by −90, −180, and −270 deg, respectively. We can see that corresponding phase shifting can be realized in the full measured frequency range just by the fast and flexible programming in the wave shaper. The change of phase shifts with the frequency indicates there are undesired delays in the phase responses, which may result from the error in the pulse shaping. By least-square fitting, these undesired delays are estimated as −4.90, −2.00, and 5.15 ps, respectively.

In conclusion, we proposed a photonic scheme to digitize RF signals with a programmable equivalent prefilter by shaping sampling pulses. The response of each channel in TIPADCs is considered as a prefilter. The conditions that the prefilter impulse response is proportional to the sampling pulse temporal shape are derived, and a method to directly control the prefilter response through shaping the sampling pulse under the conditions is found. The procedure can be considered as the sampling and reconstruction in the frequency domain to the spectrum of the sampling pulse. We experimentally demonstrated the scheme with four channels, and shifted the phase of the prefilter to validate its flexibility and reconfigurability. In theory, an ideal pulse shaping will only change the response of the prefiltering while not degrading other performances of the TIPADC. In practice, however, the loss of pulse power for the pulse shaping and the limited precision of pulse shaping may affect the performances of the TIPADC. The further optimization and calibration may be needed. These will be our next works.

Funding. National Science Foundation (NSF) (61127016, 61535006).

REFERENCES

1. G. C. Valley, Opt. Express **15**, 1955 (2007).
2. T. R. Clark, J. U. Kang, and R. D. Esman, IEEE Photon. Technol. Lett. **11**, 1168 (1999).
3. F. Coppinger, A. S. Bhushan, and B. Jalali, IEEE Trans. Microwave Theory Tech. **47**, 1309 (1999).
4. G. Wu, S. Li, X. Li, and J. Chen, Opt. Express **18**, 21162 (2010).
5. J. Capmany, J. Mora, I. Gasulla, J. Sancho, J. Lloret, and S. Sales, J. Lightwave Technol. **31**, 571 (2013).
6. F. Su, G. Wu, L. Ye, R. Liu, X. Xue, and J. Chen, Opt. Express **24**, 924 (2016).
7. A. M. Weiner, Opt. Commun. **284**, 3669 (2011).
8. J. D. McKinney and K. J. Williams, IEEE Trans. Microwave Theory Tech. **57**, 2093 (2009).